

Quantifying the structural stability of simplicial homology

Nicola Guglielmi*, Anton Savostianov†, and Francesco Tudisco†

Abstract. The homology groups of a simplicial complex reveal fundamental properties of the topology of the data or the system and the notion of topological stability naturally poses an important yet not fully investigated question. In the current work, we study the stability in terms of the smallest perturbation sufficient to change the dimensionality of the corresponding homology group. Such definition requires an appropriate weighting and normalizing procedure for the boundary operators acting on the Hodge algebra’s homology groups. Using the resulting boundary operators, we then formulate the question of structural stability as a spectral matrix nearness problem for the corresponding higher-order graph Laplacian. We develop a bilevel optimization procedure suitable for the formulated matrix nearness problem and illustrate the method’s performance on a variety of synthetic quasi-triangulation datasets and transportation networks.

Key words. simplicial complexes, homology groups, graph Laplacian, Hodge Laplacian, matrix nearness problems, matrix ODEs, spectral optimization, constrained gradient system

MSC codes. 05C50, 65F45, 65K10, 57M15, 62R40

1. Introduction. Models based on graphs and networks are ubiquitous in the sciences and engineering; for example, they have been successfully applied to model chemical reactions, traffic and electric flows, social interactions, and to describe abstract datasets in machine learning pipelines. Graph properties can be used to determine important nodes [18, 37, 13], reveal modular structure of a system [16, 36, 27], model collective network dynamics such as synchronization [31] and opinion formation [19]. However, models based on graphs are limited to descriptions based on pairwise node-node relationships.

While graph-based models are widely used and successful, many complex systems and datasets are better described by higher-order relations that go beyond pairwise interactions [4, 7, 9]. Relational data is full of interactions that happen in groups. For example, friendship relations often involve groups that are larger than two individuals. In fact, monophily and triadic closure principles from the social sciences suggest that motifs, such as triangles, are important building blocks of relational data [1, 3, 26]. Also in the presence of point-cloud data, directly modeling higher-order data interactions has led to improvements in numerous data mining settings, including clustering [8, 17, 33], link prediction [3, 6], and ranking [5, 32, 35].

Simplicial complexes are standard higher-order network models, where simplices of different order can connect a larger number of nodes. Higher-order Laplacians are key algebraic tools that naturally correspond to a simplicial complex. Formally, these are a sequence of linear operators that generalizes the better-known graph Laplacian, obtained when only pairwise edge relations are considered. Very useful topological properties about the data are revealed by the kernels of these operators which, by the Fundamental Lemma of Homology, define a homology of the data and reveal fundamental properties such as connected components, holes, and voids.

*Gran Sasso Science Institute, L’Aquila, Italy (nicola.guglielmi@gssi.it, anton.savostianov@gssi.it, francesco.tudisco@gssi.it).

In this work, we are concerned with quantifying the stability of such homological properties. More precisely, given an initial simplicial complex, we develop a numerical method based on a suitable matrix differential equation that allows us to compute the closest simplicial complex with different homology. The precise meaning of being “close” and being “different” will be based on the structure of the specific higher-order Laplacian matrix. While a great effort has been devoted in recent years to measure the presence and persistence of simplicial homology [12, 28], very little work is available about the stability of the homology classes with respect to data perturbation.

In order to make a sound mathematical formulation of the problem we aim to solve, and of the numerical model we design for its solution, in Section 2 we review in detail the notion of homology simplicial complexes and the corresponding higher-order Laplacians. In Subsection 2.2 and Subsection 3.1 we discuss how these operators may be extended to account for weighted higher-order node relations and formulate the corresponding stability problem in Section 3 and Section 4. Then, in Section 5 and Section 6 we present our numerical method based on a two-level constrained matrix gradient flow approach. Finally, we devote Section 7 to illustrate the performance of the proposed numerical scheme on several example datasets.

2. Simplicial complexes and higher-order relations. A graph \mathcal{G} is a pair of sets $(\mathcal{V}, \mathcal{E})$, where $\mathcal{V} = \{1, \dots, n\}$ is the set of vertices and $\mathcal{E} \subset \mathcal{V} \times \mathcal{V}$ is a set of unordered pairs representing the undirected edges of \mathcal{G} . We let m denote the number of edges $\mathcal{E} = \{e_1, \dots, e_m\}$ and we assume them ordered lexicographically, with the convention that $i < j$ for any $\{i, j\} \in \mathcal{E}$. For brevity, we often write ij in place of $\{i, j\}$ to denote the edge joining i and j . Moreover, we assume no self-loops, i.e., $ii \notin \mathcal{E}$ for all $i \in \mathcal{V}$.

A graph only considers pairwise relations between the vertices. A simplicial complex \mathcal{K} is a generalization of a graph that allows us to model connections involving an arbitrary number of nodes by means of higher-order simplices. Formally, a k -th order simplex (or k -simplex, briefly) is a set of $k + 1$ vertices $\{i_0, i_1, \dots, i_k\}$ with the property that every subset of k nodes itself is a $(k - 1)$ -simplex. Any $(k - 1)$ -simplex of a k -simplex is called a *face*. The collection of all such simplices forms a simplicial complex \mathcal{K} , which therefore essentially consists of a collection of sets of vertices such that every subset of the set in the collection is in the collection itself. Thus, a graph \mathcal{G} can be thought of as the collection of 0- and 1- simplices: the 0-simplices form the nodes set of \mathcal{G} , while 1-simplices form its edges. To emphasize this analogy, in the sequel we often specify that \mathcal{K} is a simplicial complex on the vertex set \mathcal{V} .

Just like the edges of a graph, to any simplicial complex, we can associate an orientation (or ordering). To underline that an ordering has been fixed, we denote an ordered k -simplex σ using square brackets $\sigma = [i_0 \dots i_k]$. In particular, as for the case of edges, in this work, we always assume the lexicographical ordering, unless specified otherwise. That is, we assume that:

1. any k -simplex $[i_0 \dots i_k]$ in \mathcal{K} is such that $i_0 < \dots < i_k$;
2. the k -simplices $\sigma_1, \sigma_2, \dots$ of \mathcal{K} are ordered so that $\sigma_i \prec \sigma_{i+1}$ for all i , where $[i_0 \dots i_k] \prec [i'_0 \dots i'_k]$ if and only if there exists h such that $0 \leq h \leq k$, $i_j = i'_j$ for $j = 0, \dots, h$ and $i_h < i'_h$.

As for the edges, we often write $i_0 \dots i_k$ in place of $[i_0 \dots i_k]$ in this case.

2.1. Homology, boundary operators and higher-order Laplacians. Topological properties of a simplicial complex can be studied by considering boundary operators, higher-order Laplacians, and the associated homology. Here we recall these concepts trying to emphasize their matrix-theoretic flavor. To this end, we first fix some further notation and recall the notion of a real k -chain.

Definition 2.1. Assume \mathcal{K} is a simplicial complex on the vertex set \mathcal{V} . For $k \geq 0$, we denote the set of all the oriented k -th order simplices in \mathcal{K} as $\mathcal{V}_k(\mathcal{K})$ or simply \mathcal{V}_k . Thus, $\mathcal{V}_0 = \mathcal{V}$ and $\mathcal{V}_1 = \mathcal{E}$ form the underlying graph of \mathcal{K} , which we denote by $\mathcal{G}_{\mathcal{K}} = (\mathcal{V}, \mathcal{E}) = (\mathcal{V}_0, \mathcal{V}_1)$.

Definition 2.2. The formal real vector space spanned by all the elements of \mathcal{V}_k with real coefficients is denoted by $C_k(\mathcal{K})$. Any element of $C_k(\mathcal{K})$, the formal linear combinations of simplices in \mathcal{V}_k , is called a k -chain.

We remark that, in the graph-theoretic terminology, $C_0(\mathcal{K})$ is usually called the space of *vertices' states*, while $C_1(\mathcal{K})$ is usually called the space of *flows* in the graph.

The chain spaces are finite vector spaces generated by the set of k -simplices. The boundary and co-boundary operators are particular linear mappings between C_k and C_{k-1} , which in a way are the discrete analogous of high-order differential operators (and their adjoints) on continuous manifolds. The boundary operator ∂_k maps a k -simplex to an alternating sum of its $(k-1)$ -dimensional faces obtained by omitting one vertex at a time. Its precise definition is recalled below, while [Figure 1](#) provides an illustrative example of its action.

Definition 2.3. Let $k \geq 1$. Given a simplicial complex \mathcal{K} over the set \mathcal{V} , the boundary operator $\partial_k: C_k(\mathcal{K}) \mapsto C_{k-1}(\mathcal{K})$ maps every ordered k -simplex $[i_0 \dots i_k] \in C_k(\mathcal{K})$ to the following alternated sum of its faces:

$$\partial_k[i_0 \dots i_k] = \sum_{j=0}^k (-1)^j [i_0 \dots i_{j-1} i_{j+1} \dots i_k] \in C_{k-1}(\mathcal{K})$$

As we assume the k -simplices in \mathcal{V}_k are ordered lexicographically, we can fix a canonical basis for $C_k(\mathcal{K})$ and we can represent ∂_k as a matrix B_k with respect to such basis. In fact, once the ordering is fixed, $C_k(\mathcal{K})$ is isomorphic to $\mathbb{R}^{\mathcal{V}_k}$, the space of functions from \mathcal{V}_k to \mathbb{R} or, equivalently, the space of real vectors with $|\mathcal{V}_k|$ entries. Thus, B_k is a $|\mathcal{V}_{k-1}| \times |\mathcal{V}_k|$ matrix and ∂_k^* coincides with B_k^\top . We shall always assume the canonical basis for $C_k(\mathcal{K})$ is fixed in this way and we will deal exclusively with the matrix representation B_k from now on. An example of B_k for $k=1$ and $k=2$ is shown in [Figure 1](#).

A direct computation shows that the following fundamental identity holds (see e.g. [\[24, Thm. 5.7\]](#))

$$(2.1) \quad B_k B_{k+1} = 0$$

for any k . This identity is also known in the continuous case as the Fundamental Lemma of Homology and it allows us to define a homology group associated with each k -chain. In fact, [\(2.1\)](#) implies in particular that $\text{im } B_{k+1} \subset \ker B_k$, so that the k -th homology group is correctly defined:

$$\mathcal{H}_k := \ker B_k / \text{im } B_{k+1}$$

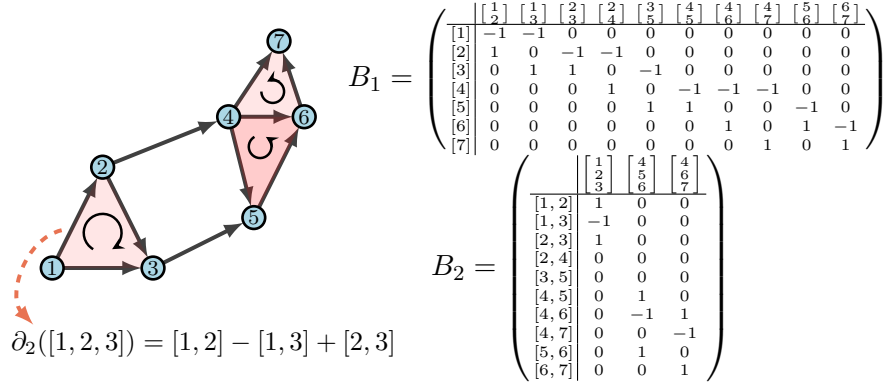


Figure 1. Left-hand side panel: example of simplicial complex \mathcal{K} on 7 nodes, and of the action of ∂_2 on the 2-simplex $[1, 2, 3]$; 2-simplices included in the complex are shown in red, arrows correspond to the orientation. Panels on the right: matrix forms B_1 and B_2 of boundary operators ∂_1 and ∂_2 respectively.

The dimensionality of the k -th homology group is known as k -th Betti's number $\beta_k = \dim \mathcal{H}_k$, while the elements of \mathcal{H}_k correspond to so-called k -dimensional holes in the simplicial complex. For example, \mathcal{H}_0 , \mathcal{H}_1 and \mathcal{H}_2 describe *connected components*, *holes* and *three-dimensional voids* respectively. By standard algebraic passages one sees that \mathcal{H}_k is isomorphic to $\ker(B_k^\top B_k + B_{k+1}^\top B_{k+1})$. Thus, the number of k -dimensional holes corresponds to the dimension of the kernel of a linear operator, which is known as k -th order Laplacian or *higher-order Laplacian* of the simplicial complex \mathcal{K} .

Definition 2.4. Given a simplicial complex \mathcal{K} and the boundary operators B_k and B_{k+1} , the k -th order Laplacian L_k of \mathcal{K} is the $|\mathcal{V}_k| \times |\mathcal{V}_k|$ matrix defined as:

$$(2.2) \quad L_k = B_k^\top B_k + B_{k+1}^\top B_{k+1}$$

In particular, we remark that:

- the 0-order Laplacian is the standard *combinatorial graph Laplacian* $L_0 = B_1 B_1^\top \in \mathbb{R}^{n \times n}$, whose diagonal entries consist of the degrees of the corresponding vertices (i.e. the number of 1-simplices each vertex belongs to), while the off-diagonal $(L_0)_{ij}$ is equal to -1 if either ij is a 1-simplex, and it is zero otherwise;
- the 1-order Laplacian is known as *Hodge Laplacian* $L_1 = B_1^\top B_1 + B_2^\top B_2 \in \mathbb{R}^{m \times m}$. Similarly to the 0-order case L_0 , one can describe the entries of L_1 in terms of the structure of the simplicial complex, see e.g. [25].

2.1.1. Connected components and holes. The boundary operators B_k on \mathcal{K} are directly connected with discrete notions of differential operators on the graph. In particular, B_1 , B_1^\top , and B_2^\top are the graph's divergence, gradient, and curl operators, respectively. We refer to [24] for more details. As \mathcal{H}_k is isomorphic to $\ker L_k$, we have that the following *Hodge decomposition* of $\mathbb{R}^{\mathcal{V}_k}$ holds

$$\mathbb{R}^{\mathcal{V}_k} = \text{im } B_{k+1} \oplus \text{im } B_k^\top \oplus \ker L_k = \text{im } \bar{B}_{k+1} \oplus \text{im } \bar{B}_k^\top \oplus \ker \bar{L}_k.$$



Figure 2. Continuous and analogous discrete manifolds with one 1-dimensional hole ($\dim \overline{\mathcal{H}}_1 = 1$). Left pane: the continuous manifold; center pane: the discretization with mesh vertices; right pane: a simplicial complex built upon the mesh. Triangles in the simplicial complex \mathcal{K} are colored gray (right).

Thus, the space of vertex states $\mathbb{R}^{\mathcal{V}_0}$ can be decomposed as $\mathbb{R}^{\mathcal{V}_0} = \text{im } B_1 \oplus \ker L_0$, the sum of divergence-free vectors and harmonic vectors, which correspond to the connected components of the graph. In particular, for a connected graph, $\ker L_0$ is one-dimensional and consists of entry-wise constant vectors. Thus, for a connected graph, $\text{im } B_1$ is the set of vectors whose entries sum up to zero.

Similarly, the space of flows on graph's edges $\mathbb{R}^{\mathcal{V}_1}$ can be decomposed as $\mathbb{R}^{\mathcal{V}_1} = \text{im } B_2 \oplus \text{im } B_1^\top \oplus \ker L_1$. Thus, each flow can be decomposed into its gradient part $\text{im } B_1^\top$, which consists of flows with zero cycle sum, its curl part $\text{im } B_2$, which consists of circulations around order-2 simplicies in \mathcal{K} , and its harmonic part $\ker L_1$, which represents 1-dimensional holes defined as global circulations modulo the curl flows.

While 0-dimensional holes are easily understood as the connected components of the graph $\mathcal{G}_\mathcal{K}$, a notion of “holes in the graph” $\mathcal{G}_\mathcal{K}$ corresponds to 1-dimensional holes in \mathcal{K} . This terminology comes from the analogy with the continuous case. In fact, if the graph is obtained as a discretization of a continuous manifold, harmonic functions in the homology group \mathcal{H}_1 would correspond to the holes in the manifold, as illustrated in Figure 2. Moreover, the Hodge Laplacian of a simplicial complex built on N randomly sampled points in the manifold converges in the thermodynamic limit to its continuous counterpart, as $N \rightarrow \infty$, [11].

2.2. Normalized and weighted higher-order Laplacians. In the classical graph setting, a normalized and weighted version of the Laplacian matrix is very often employed in applications. From a matrix theoretic point of view, having a weighted graph corresponds to allowing arbitrary nonnegative entries in the adjacency matrix defining the graph. In terms of boundary operators, this coincides with a positive diagonal rescaling. Analogously, the normalized Laplacian is defined by applying a diagonal congruence transformation to the standard Laplacian using the node weights. We briefly review these two constructions below.

Let $\mathcal{G} = (\mathcal{V}, \mathcal{E})$ be a graph with positive node and edge weight functions $w_0 : \mathcal{V} \rightarrow \mathbb{R}_{++}$ and $w_1 : \mathcal{E} \rightarrow \mathbb{R}_{++}$, respectively. Define the $|\mathcal{V}| \times |\mathcal{V}|$ and $|\mathcal{E}| \times |\mathcal{E}|$ diagonal matrices $W_0 = \text{Diag}\{w_0(v_i)^{1/2}\}_{i=1}^n$ and $W_1 = \text{Diag}\{w_1(e_i)^{1/2}\}_{i=1}^m$. Then $\overline{B}_1 = W_0^{-1} B_1 W_1$ is the normalized and weighted boundary operator of \mathcal{G} and we have that

$$(2.3) \quad \overline{L}_0 = \overline{B}_1 \overline{B}_1^\top = W_0^{-1} B_1 W_1^2 B_1^\top W_0^{-1}$$

is the normalized weighted graph Laplacian of \mathcal{G} .

In particular, note that, as for L_0 , the entries of \overline{L}_0 uniquely characterize the graph

topology, in fact we have

$$(\bar{L}_0)_{ii} = \frac{\deg(i)}{w_0(i)}, \quad (\bar{L}_0)_{ij} = \begin{cases} -\frac{w_1(ij)}{\sqrt{w_0(i)w_0(j)}} & ij \in \mathcal{E} \\ 0 & \text{otherwise} \end{cases}, \text{ for } i \neq j$$

where $\deg(i)$ denotes the (weighted) degree of node i , i.e. $\deg(i) = \sum_{e \in \mathcal{E}: i \in e} w_1(e)$.

While the definition of k -th order Laplacian is well-established for the case of unweighted edges and simplices, a notion of weighted and normalized k -th order Laplacian is not universally available and it might depend on the application one has at hand. For example, different definitions of weighted Hodge Laplacian are considered in [10, 22, 24, 29].

At the same time, we notice that the notation used in (2.3) directly generalizes to higher orders. Thus, we propose the following notion of normalized and weighted k -th Laplacian

Definition 2.5. Let \mathcal{K} be a simplicial complex and let $w_k : \mathcal{V}_k \rightarrow \mathbb{R}_{++}$ be a positive-valued weight function on the k -simplices of \mathcal{K} . Define the diagonal matrix $W_k = \text{Diag}\{w_k(\sigma_i)^{1/2}\}_{i=1}^{|\mathcal{V}_k|}$. Then, $\bar{B}_k = W_{k-1}^{-1} B_k W_k$ is the normalized and weighted k -th boundary operator, to which corresponds the normalized and weighted k -th Laplacian

$$(2.4) \quad \begin{aligned} \bar{L}_k &= \bar{B}_k^\top \bar{B}_k + \bar{B}_{k+1} \bar{B}_{k+1}^\top \\ &= W_k B_k^\top W_{k-1}^{-2} B_k W_k + W_k^{-1} B_{k+1} W_{k+1}^2 B_{k+1}^\top W_k^{-1}. \end{aligned}$$

Note that, from the definition $\bar{B}_k = W_{k-1}^{-1} B_k W_k$ and (2.1), we immediately have that $\bar{B}_k \bar{B}_{k+1} = 0$. Thus, the group $\bar{\mathcal{H}}_k = \ker \bar{B}_k / \text{im } \bar{B}_{k+1}$ is well defined for any choice of positive weights w_k and is isomorphic to $\ker \bar{L}_k$. While the homology group may depend on the weights, we observe below that its dimension does not. Precisely, we have

Proposition 2.6. The dimension of the homology groups of \mathcal{K} is not affected by the weights of its k -simplices. Precisely, if W_k are positive diagonal matrices, we have

$$(2.5) \quad \dim \ker \bar{B}_k = \dim \ker B_k, \quad \dim \ker \bar{B}_k^\top = \dim \ker B_k^\top, \quad \dim \bar{\mathcal{H}}_k = \dim \mathcal{H}_k.$$

Moreover, $\ker B_k = W_k \ker \bar{B}_k$ and $\ker B_k^\top = W_{k-1}^{-1} \ker \bar{B}_k^\top$.

Proof. Since W_k is an invertible diagonal matrix,

$$\bar{B}_k \mathbf{x} = 0 \iff W_{k-1}^{-1} B_k W_k \mathbf{x} = 0 \iff B_k W_k \mathbf{x} = 0.$$

Hence, if $\mathbf{x} \in \ker \bar{B}_k$, then $W_k \mathbf{x} \in \ker B_k$, and, since W_k is bijective, $\dim \ker \bar{B}_k = \dim \ker B_k$. Similarly, one observes that $\dim \ker \bar{B}_k^\top = \dim \ker B_k^\top$.

Moreover, since $\bar{B}_k \bar{B}_{k+1} = 0$, then $\text{im } \bar{B}_{k+1} \subseteq \ker \bar{B}_k$ and $\text{im } \bar{B}_k^\top \subseteq \ker \bar{B}_{k+1}^\top$. This yields $\ker \bar{B}_k \cup \ker \bar{B}_{k+1}^\top = \mathbb{R}^{\mathcal{V}_k} = \ker B_k \cup \ker B_{k+1}^\top$. Thus, for the homology group it holds:

$$\begin{aligned} \dim \bar{\mathcal{H}}_k &= \dim \left(\ker \bar{B}_k \cap \ker \bar{B}_{k+1}^\top \right) = \\ &= \dim \ker \bar{B}_k + \dim \ker \bar{B}_{k+1}^\top - \dim \left(\ker \bar{B}_k \cup \ker \bar{B}_{k+1}^\top \right) = \\ &= \dim \ker B_k + \dim \ker B_{k+1}^\top - \dim \left(\ker B_k \cup \ker B_{k+1}^\top \right) = \dim \mathcal{H}_k \end{aligned} \quad \blacksquare$$

2.3. Principal spectral inheritance. Before moving on to the next section, we recall here a relatively direct but important spectral property that connects the spectra of the k -th and $(k + 1)$ -th order Laplacians.

Theorem 2.7 (HOL's spectral inheritance). *Let L_k and L_{k+1} be higher-order Laplacians for the same simplicial complex \mathcal{K} . Let $\bar{L}_k = \bar{L}_k^{\text{down}} + \bar{L}_k^{\text{up}}$, where $\bar{L}_k^{\text{down}} = \bar{B}_k^\top \bar{B}_k$ and $\bar{L}_k^{\text{up}} = \bar{B}_{k+1} \bar{B}_{k+1}^\top$. Then:*

1. $\sigma_+(\bar{L}_k^{\text{up}}) = \sigma_+(\bar{L}_{k+1}^{\text{down}})$, where $\sigma_+(\cdot)$ denotes the positive part of the spectrum;
2. if $0 \neq \mu \in \sigma_+(\bar{L}_k^{\text{up}}) = \sigma_+(\bar{L}_{k+1}^{\text{down}})$, then the eigenvectors are related as follows:
 - (a) if \mathbf{x} is an eigenvector for \bar{L}_k^{up} with the eigenvalue μ , then $\mathbf{y} = \frac{1}{\sqrt{\mu}} \bar{B}_{k+1}^\top \mathbf{x}$ is an eigenvector for $\bar{L}_{k+1}^{\text{down}}$ with the same eigenvalue;
 - (b) if \mathbf{u} is an eigenvector for $\bar{L}_{k+1}^{\text{down}}$ with the eigenvalue μ and $\mathbf{u} \notin \ker \bar{B}_{k+1}$, then $\mathbf{v} = \frac{1}{\sqrt{\mu}} \bar{B}_{k+1} \mathbf{u}$ is an eigenvector for \bar{L}_k^{up} with the same eigenvalue;
3. for each Laplacian \bar{L}_k : if $\mathbf{v} \notin \ker \bar{L}_k^{\text{down}}$ is the eigenvector for \bar{L}_k^{down} , then $\mathbf{v} \in \ker \bar{L}_k^{\text{up}}$; vice versa, if $\mathbf{u} \notin \ker \bar{L}_k^{\text{up}}$ is the eigenvector for \bar{L}_k^{up} , then $\mathbf{v} \in \ker \bar{L}_k^{\text{down}}$;
4. consequently, there exist $\mu \in \sigma_+(\bar{L}_k)$ with an eigenvector $\mathbf{u} \in \ker \bar{L}_k^{\text{up}}$, and $\nu \in \sigma_+(\bar{L}_{k+1})$ with an eigenvector $\mathbf{u} \in \ker \bar{L}_{k+1}^{\text{down}}$, such that:

$$\bar{B}_k^\top \bar{B}_k \mathbf{v} = \mu \mathbf{v}, \quad \bar{B}_{k+2} \bar{B}_{k+2}^\top \mathbf{u} = \nu \mathbf{u}.$$

Proof. For (2a) it is sufficient to note that $\bar{L}_{k+1}^{\text{down}} \mathbf{y} = \bar{B}_{k+1}^\top \bar{B}_{k+1} \frac{1}{\sqrt{\mu}} \bar{B}_{k+1}^\top \mathbf{x} = \frac{1}{\sqrt{\mu}} \bar{B}_{k+1}^\top \bar{L}_k^{\text{up}} \mathbf{x} = \sqrt{\mu} \bar{B}_{k+1}^\top \mathbf{x} = \mu \mathbf{y}$. Similarly, for (2b): $\bar{L}_k^{\text{up}} \mathbf{v} = \bar{B}_{k+1} \bar{B}_{k+1}^\top \frac{1}{\sqrt{\mu}} \bar{B}_{k+1} \mathbf{u} = \frac{1}{\sqrt{\mu}} \bar{B}_{k+1} \bar{L}_{k+1}^{\text{down}} \mathbf{u} = \mu \mathbf{v}$; joint 2(a) and 2(b) yield (1). Hodge decomposition immediately yields the strict separation of eigenvectors between \bar{L}_k^{up} and \bar{L}_k^{down} , (3); given (3), all the inherited eigenvectors from (2a) fall into the $\ker \bar{L}_{k+1}^{\text{down}}$, thus resulting into (4). ■

In other words, the variation of the spectrum of the k -th Laplacian when moving from one order to the next one works as follows: the down-term $\bar{L}_{k+1}^{\text{down}}$ inherits the positive part of the spectrum from the up-term of \bar{L}_k^{up} ; the eigenvectors corresponding to the inherited positive part of the spectrum lie in the kernel of $\bar{L}_{k+1}^{\text{up}}$; at the same time, the “new” up-term $\bar{L}_{k+1}^{\text{up}}$ has a new, non-inherited, part of the positive spectrum (which, in turn, lies in the kernel of the $(k + 2)$ -th down-term).

In particular, we notice that for $k = 0$, since $B_0 = 0$ and $\bar{L}_0 = \bar{L}_0^{\text{up}}$, the theorem yields $\sigma_+(\bar{L}_0) = \sigma_+(\bar{L}_1^{\text{down}}) \subseteq \sigma_+(\bar{L}_1)$. In other terms, the positive spectrum of the \bar{L}_0 is inherited by the spectrum of \bar{L}_1 and the remaining (non-inherited) part of $\sigma_+(\bar{L}_1)$ coincides with $\sigma_+(\bar{L}_1^{\text{up}})$. Figure 3 provides an illustration of the statement of Theorem 2.7 for $k = 0$.

3. Problem setting: Nearest complex with different homology. Suppose we are given a simplicial complex \mathcal{K} on the vertex set \mathcal{V} , with simplex weight functions w_0, w_1, \dots , and let $\beta_k = \dim \mathcal{H}_k = \dim \bar{\mathcal{H}}_k$ the dimension of its k -homology. We aim at finding the closest simplex on the same vertex set \mathcal{V} , with a strictly larger number of holes. As it is the most frequent higher-order Laplacian appearing in applications and since this provides already a

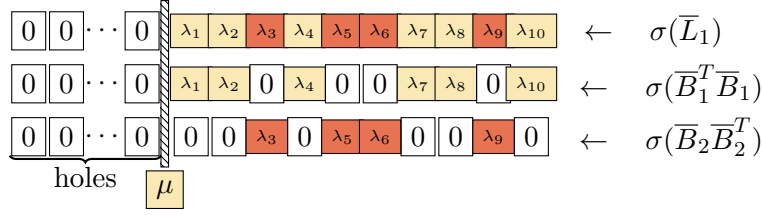


Figure 3. Illustration for the principal spectrum inheritance ([Theorem 2.7](#)) in case $k = 0$: spectra of \bar{L}_1 , \bar{L}_1^{down} and \bar{L}_1^{up} are shown. Colors signify the splitting of the spectrum, $\lambda_i > 0 \in \sigma(\bar{L}_1)$; all yellow eigenvalues are inherited from $\sigma_+(\bar{L}_0)$; red eigenvalues belong to the non-inherited part. Dashed barrier μ signifies the penalization threshold (see the target functional in [Section 4](#)) preventing homological pollution (see [Subsection 3.1](#)).

large number of numerical complications, we focus here only on the Hodge Laplacian case: given the simplicial complex $\mathcal{K} = (\mathcal{V}_0, \mathcal{V}_1, \mathcal{V}_2, \dots)$, we look for the smallest perturbation of the edges \mathcal{V}_1 which increases the dimension of \mathcal{H}_1 . More precisely:

Problem 3.1. Let \mathcal{K} be a simplicial complex of order at least 2 with edge weights w_1 and corresponding diagonal weight matrix W_1 , and let $\beta_1(W_1)$ be the dimension of the homology group corresponding to the weights W_1 . For $\varepsilon > 0$, let

$$\Omega(\varepsilon) = \left\{ \text{diagonal matrices } W \text{ such that } \|W\| = \varepsilon \right\},$$

$$\Pi(W_1) = \left\{ \text{diagonal matrices } W \text{ such that } W_1 + W \geq 0 \right\}.$$

In other words, $\Omega(\varepsilon)$ is an ε -sphere and $\Pi(W_1)$ allows only non-negative simplex weights. We look for the smallest perturbation ε such that there exists a weight modification $\delta W_1 \in \Omega(\varepsilon) \cap \Pi(W_1)$ such that $\beta_1(W_1) < \beta_1(W_1 + \delta W_1)$.

Here, and throughout the paper, $\|X\|$ denotes either the Frobenius norm if X is a matrix, or the Euclidean norm if X is a vector. Note that, as we are looking for the smallest ε , the equality $\|W\| = \varepsilon$ is an obvious choice, as opposed to $\|W\| \leq \varepsilon$.

As the dimension β_1 coincides with the kernel of \bar{L}_1 , we approach this problem through the minimization of a functional based on the spectrum of the 0-th and 1-st Laplacian of the simplicial complex. In order to define such functional, we first make a number of considerations.

Note that, due to [Proposition 2.6](#), the dimension of the first homology group does not change when the edge weights are perturbed, as long as all the weights remain positive. Thus, in order to find the desired perturbation δW_1 , we need to set some of the initial weights to zero. This operation creates several potential issues we need to carefully address, as discussed next.

First, setting an edge to zero implies that one is formally removing that edge from the simplicial complex. As the simplicial complex structure needs to be maintained, when doing so we need to set to zero also the weight of any 2-simplex that contains that edge. For this reason, if $\tilde{w}_1(e) = w_1(e) + \delta w_1(e)$ is the new edge weight function, we require the weight function of the 2-simplices to change into \tilde{w}_2 , defined as

$$\tilde{w}_2(i_1 i_2 i_3) = f \left(\frac{\delta w_1(i_1 i_2)}{w_1(i_1 i_2)}, \frac{\delta w_1(i_2 i_3)}{w_1(i_2 i_3)}, \frac{\delta w_1(i_1 i_3)}{w_1(i_1 i_3)} \right) \cdot w_2(i_1 i_2 i_3)$$

where $f(u_1, u_2, u_3)$ is a function such that $f(0, 0, 0) = 1$ and that monotonically decreases to zero as $u_i \rightarrow -1$, for any $i = 1, 2, 3$. An example of such f is

$$(3.1) \quad f(u_1, u_2, u_3) = 1 - \min\{u_1, u_2, u_3\}.$$

Second, when setting the weight of an edge to zero we may disconnect the underlying graph and create an all-zero column and row in the Hodge Laplacian. This gives rise to the phenomenon that we call “homological pollution”, which we will discuss in detail in the next subsection.

3.1. Homological pollution: inherited almost disconnectedness. As the Hodge homology β_1 corresponds to the number of zero eigenvalues in $\ker \bar{L}_1$, the intuition suggests that if \bar{L}_1 has some eigenvalue that is close to zero, then the simplicial complex is “close to” having at least one more 1-dimensional hole. There are a number of problems with this intuitive consideration.

By [Theorem 2.7](#) for $k = 0$, $\sigma_+(\bar{L}_1)$ inherits $\sigma_+(\bar{L}_0)$. Hence, if the weights in W_1 vary continuously so that a positive eigenvalue in $\sigma_+(\bar{L}_0)$ approaches 0, the same happens to $\sigma_+(\bar{L}_1)$. Assuming the initial graph \mathcal{G}_K is connected, an eigenvalue that approaches zero in $\sigma_+(\bar{L}_0)$ would imply that \mathcal{G}_K is approaching disconnectedness. This leads to a sort of *pollution* of the kernel of \bar{L}_1 as an almost-zero eigenvalue which corresponds to an “almost” 0-dimensional hole (disconnected component) from \bar{L}_0 is inherited into the spectrum of \bar{L}_1 , but this small eigenvalue of \bar{L}_1 does not correspond to the creation of a new 1-dimensional hole in the reduced complex.

To better explain the problem of homological pollution, let us consider the following illustrative example.

Example 3.2. Consider the simplicial complex of order 2 depicted in [Figure 4a](#). In this example we have $\mathcal{V}_0 = \{1, \dots, 7\}$, $\mathcal{V}_1 = \{[1, 2], [1, 3], [2, 3], [2, 4], [3, 5], [4, 5], [4, 6], [5, 6], [5, 7], [6, 7]\}$ and $\mathcal{V}_2 = \{[1, 2, 3], [4, 5, 6], [5, 6, 7]\}$, all with weight equal to one: $w_k \equiv 1$ for $k = 0, 1, 2$. The only existing 1-dimensional hole is shown in red and thus the corresponding Hodge homology is $\beta = 1$. Now, consider perturbing the weight of edges $[2, 4]$ and $[3, 5]$ by setting their weights to $\varepsilon > 0$ [Figure 4b](#). For small ε , this perturbation implies that the smallest nonzero eigenvalue μ_2 in $\sigma_+(\bar{L}_0)$ is scaled by ε . As $\sigma_+(\bar{L}_0) \subseteq \sigma_+(\bar{L}_1)$, we have that $\dim \ker \bar{L}_1 = 1$ and $\sigma_+(\bar{L}_1)$ has an arbitrary small eigenvalue, approaching 0 with $\varepsilon \rightarrow 0$. At the same time, when $\varepsilon \rightarrow 0$, the reduced complex obtained by removing the zero edges as in [Figure 4c](#) does not have any 1-dimensional hole, i.e. $\beta_1 = 0$. Thus, in this case, the presence of a very small eigenvalue $\mu_2 \in \sigma_+(\bar{L}_1)$ does not imply that the simplicial complex is close to a simplicial complex with a larger Hodge homology.

To mitigate the phenomenon of homological pollution, in our spectral-based functional for [Problem 3.1](#) we include a term that penalizes the spectrum of \bar{L}_0 from approaching zero. To this end, we observe below that a careful choice of the vertex weights is required.

The smallest non-zero eigenvalue of the Laplacian $\mu_2 \in \sigma(\bar{L}_0)$ is directly related to the connectedness of the graph \mathcal{G}_K . This relation is well-known and dates back to the pioneering work of Fiedler [\[14\]](#). In particular, as μ_2 is a function of node and edge weights, the following

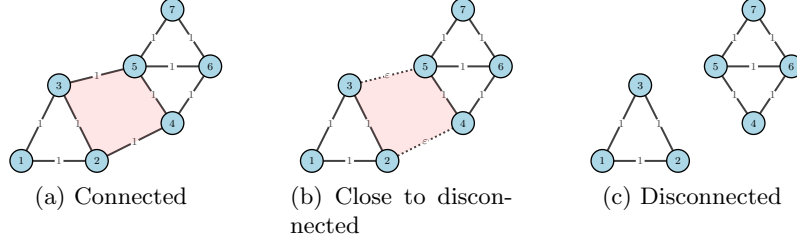


Figure 4. Example of the homological pollution, [Example 3.2](#), for the simplicial complex \mathcal{K} on 7 vertices; the existing hole is shown in red (left and center pane), all 3 cliques are included in the simplicial complex. The left pane demonstrates the initial setup with 1 hole; the center pane retains the hole exhibiting spectral pollution; the continuous transition to the eliminated edges with $\beta_1 = 0$ (no holes) is shown on the right pane.

generalized version of the Cheeger inequality holds (see e.g. [\[34\]](#))

$$(3.2) \quad \frac{1}{2} \mu_2 \leq h(\mathcal{G}_{\mathcal{K}}) \leq \left(2 \mu_2 \max_{i \in \mathcal{V}_0} \frac{\deg(i)}{w_0(i)} \right)^{1/2},$$

where

$$h(\mathcal{G}_{\mathcal{K}}) = \min_{S \subset \mathcal{V}_0} \frac{w_1(S, \mathcal{V}_0 \setminus S)}{\min\{w_0(S), w_0(\mathcal{V}_0 \setminus S)\}},$$

with

$$w_1(S, \mathcal{V}_0 \setminus S) = \sum_{ij \in \mathcal{V}_1: i \in S, j \notin S} w_1(ij), \quad \deg(i) = \sum_{j: ij \in \mathcal{V}_1} w_i(ij), \quad w_0(S) = \sum_{i \in S} w_0(i).$$

We immediately see from (3.2) that when the graph $\mathcal{G}_{\mathcal{K}}$ is disconnected, then $h(\mathcal{G}_{\mathcal{K}}) = 0$ and $\mu_2 = 0$ as well. Vice-versa, if μ_2 goes to zero, then $h(\mathcal{G}_{\mathcal{K}})$ decreases to zero too. While this happens independently of the choice of w_0 and w_1 , if w_0 is a function of w_1 then it might fail to capture the presence of edges whose weight is decreasing and is about to disconnect the graph.

To see this, consider the example choice $w_0(i) = \deg(i)$, the degree of node i in $\mathcal{G}_{\mathcal{K}}$. Note that this is a very common choice in the graph literature, with several useful properties, including the fact that no other graph-dependent constant appears in the Cheeger inequality (3.2) other than μ_2 . For this weight choice, consider the case of a leaf node, a node $i \in \mathcal{V}_0$ that has only one edge $ij_0 \in \mathcal{V}_1$ connecting i to the rest of the (connected) graph $\mathcal{G}_{\mathcal{K}}$ via the node j_0 . If we set $w_1(ij_0) = \varepsilon$ and we let ε decrease to zero, the graph $\mathcal{G}_{\mathcal{K}}$ is approaching disconnectedness and we would expect $h(\mathcal{G}_{\mathcal{K}})$ and μ_2 to decrease as well. However, one easily verifies that both μ_2 and $h(\mathcal{G}_{\mathcal{K}})$ are constant with respect to ε in this case, as long as $\varepsilon \neq 0$.

In order to avoid such a discontinuity, in our weight perturbation strategy for the simplex \mathcal{K} , if w_0 is a function of w_1 , we perturb it by a constant shift. Precisely, if w_0 is the initial vertex weight of \mathcal{K} , we set $\tilde{w}_0(i) = w_0(i) + \varrho$, with $\varrho > 0$. So, for example, if $w_0 = \deg$ and the new edge weight function $\tilde{w}_1(e) = w_1(e) + \delta w_1(e)$ is formed after the addition of δW_1 , we set $\tilde{w}_0(i) = \sum_j [w_1(ij) + \delta w_1(ij)] + \varrho$.

4. Spectral functional for 1-st homological stability. We are now in the position to formulate our proposed spectral-based functional, whose minimization leads to the desired small perturbation that changes the first homology of \mathcal{K} . In the notation of [Problem 3.1](#), we are interested in the smallest perturbation ε and the corresponding modification $\delta W_1 \in \Omega(\varepsilon) \cap \Pi(W_1)$ that increases β_1 .

As $\|\delta W_1\| = \varepsilon$, for convenience we indicate $\delta W_1 = \varepsilon E$ with $\|E\| = 1$ so $E \in \Omega(1) \cap \Pi_\varepsilon(W_1)$, where $\Pi_\varepsilon(W_1) = \{W \mid \varepsilon W \in \Pi(W_1)\}$. For the sake of simplicity, we will omit the dependencies and write Ω and Π_ε , when there is no danger of ambiguity. Finally, let us denote by $\beta_1(\varepsilon, E)$ the first Betti number corresponding to the simplicial complex perturbed via the edge modification εE . With this notation, we can reformulate [Problem 3.1](#) as follows:

Problem 4.1. *Find the smallest $\varepsilon > 0$, such that there exists an admissible perturbation $E \in \Omega \cap \Pi_\varepsilon$ with an increased number of holes, i.e.*

$$(4.1) \quad \min \{ \varepsilon > 0 : \beta_1(\varepsilon, E) \geq \beta_1 + 1 \text{ for some } E \in \Omega \cap \Pi_\varepsilon \}$$

where $\beta_1 = \beta_1(0, \cdot)$ is the first Betti number of the original simplicial complex.

In order to approach [Problem 4.1](#), we introduce a target functional $F(\varepsilon, E)$, based on the spectrum of the 1-Laplacian $\bar{L}_1(\varepsilon, E)$ and the 0-Laplacian $\bar{L}_0(\varepsilon, E)$, where the dependence on ε and E is to emphasize the corresponding weight perturbation is of the form $W_1 \mapsto W_1 + \varepsilon E$.

Our goal is to move a positive entry in $\sigma_+(\bar{L}_1(\varepsilon, E))$ into the kernel. At the same time, assuming the initial graph $\mathcal{G}_\mathcal{K}$ is connected, one should avoid the inherited almost disconnectedness with small positive entries of $\sigma_+(\bar{L}_0(\varepsilon, E))$. As, by [Theorem 2.7](#) for $k = 0$, $\sigma_+(\bar{L}_0(\varepsilon, E)) = \sigma_+(\bar{L}_1^{\text{down}}(\varepsilon, E))$, the only eigenvalue of $\bar{L}_1(\varepsilon, E)$ that can be continuously driven to 0 comes from $\bar{L}_1^{\text{up}}(\varepsilon, E)$. For this reason, let us denote the *first non-zero eigenvalue* of the up-Laplacian $\bar{L}_1^{\text{up}}(\varepsilon, E)$ by $\lambda_+(\varepsilon, E)$. The proposed target functional $F(\varepsilon, E)$ is defined as:

$$(4.2) \quad F(\varepsilon, E) = \frac{\lambda_+(\varepsilon, E)^2}{2} + \frac{\alpha}{2} \max \left(0, 1 - \frac{\mu_2(\varepsilon, E)}{\mu} \right)^2$$

where α and μ are positive parameters, and $\mu_2(\varepsilon, E)$ is the first nonzero eigenvalue of $\bar{L}_0(\varepsilon, E)$. As recalled in [Subsection 3.1](#), $\mu_2(\varepsilon, E)$ is an algebraic measure of the connectedness of the perturbed graph, thus the whole second term in (4.2) “activates” when such algebraic connectedness falls below the threshold μ .

By design, $F(\varepsilon, E)$ is non-negative and is equal to 0 iff $\lambda_+(\varepsilon, E)$ reaches 0, increasing the dimension of \mathcal{H}_1 . Using this functional, we recast the [Problem 4.1](#) as

$$(4.3) \quad \min \{ \varepsilon > 0 : F(\varepsilon, E) = 0 \text{ for some } E \in \Omega_\varepsilon \}$$

Remark 4.2. When $\mathcal{G}_\mathcal{K}$ is connected, $\dim \ker \bar{L}_0 = 1$ and by [Theorem 2.7](#) $\dim \ker \bar{L}_1^{\text{up}} = \dim \ker \bar{L}_1 + (n - \dim \ker \bar{L}_0) = n + \beta_1 - 1$, so the first nonzero eigenvalue of \bar{L}_1^{up} is the $(n + \beta_1)$ -th. While $(n + \beta_1)$ can be a large number in practice, we will discuss in [Subsection 6.1](#) an efficient method that allows us to compute $\lambda_+(\varepsilon, E)$ without computing any of the previous $(n + \beta_1 - 1)$ eigenvalues.

5. A two-level optimization procedure. We propose to approach (4.3) by means of a two-level iterative method, which is based on the successive minimization of the target functional $F(\varepsilon, E)$ and a subsequent tuning of the parameter ε . More precisely, we propose the following two-level scheme. A similar procedure was used in the context of graph spectral nearness in [2] and in other matrix nearness problems [21].

1. **Inner level:** for fixed $\varepsilon > 0$, solve the minimization problem

$$E(\varepsilon) = \arg \min_{E \in \Omega \cap \Pi_\varepsilon} F(\varepsilon, E)$$

by a constrained gradient flow which we formulate below, where we denote the computed minimizer by $E(\varepsilon)$.

2. **Outer level:** given the function $\varepsilon \mapsto E(\varepsilon)$, we consider the optimization problem:

$$(5.1) \quad F(\varepsilon, E(\varepsilon)) = 0$$

and look for the smallest value $\varepsilon^* > 0$ that solves (5.1).

Details on the implementation of both levels are given below.

By construction, the resulting algorithm converges to a minimum of $F(\varepsilon, E)$. Although global convergence to the global optimum is not guaranteed, in our experiments we always observe the method reaches the expected global solution. However, we point out that there exists one pathological configuration of the simplicial complex \mathcal{K} which would prevent global optimality. This happens when there are several holes and simplices from $\mathcal{V}_2(\mathcal{K})$ being adjacent to each other only through a common edge, which has a small weight. In that case, the algorithm would always eliminate that common edge, whilst the correctness of this answer would depend on the balance between the number of holes and adjacent simplices. These configurations are rarely present in real-life systems (we did not encounter them in any of our tests); nevertheless, one can tackle such unsuccessful runs through manual weight modification of the undesired edge.

5.1. Inner Level Iteration. Here we consider the minimization problem with respect to E and fixed scalar parameters: the perturbation norm ε is inherited from the outer level, and the connectedness parameters α and μ are assumed to be given (we will discuss the choice of μ and α later).

We solve the resulting minimization problem $\min\{F(\varepsilon, E) : E \in \Omega \cap \Pi_\varepsilon\}$ by solving the associated constrained gradient system

$$(5.2) \quad \dot{E}(t) = -\mathbb{P}_{\Omega \cap \Pi_\varepsilon} G(\varepsilon, E(t))$$

where $G(\varepsilon, E) = \nabla_E F_k(\varepsilon, E)$ and $\mathbb{P}_{\Omega \cap \Pi_\varepsilon}$ is a projector onto the admissible set $\Omega \cap \Pi_\varepsilon$ (where ε is fixed). Since the system integrates the anti-gradient, a minimizer (at least local) of $F(\varepsilon, E)$ is obtained at $t \rightarrow \infty$. Equation (5.2) introduces a dummy time dependence outlining the difference between the discrete gradient descent and the gradient flow. In the current work, we use the latter which benefits from a variety of known integrators and simpler implementation of constraints.

We devote the next two Subsection 5.2 and Subsection 5.3 to computing the projected gradient in (5.2). The idea is to express the derivative of F in terms of the derivative of the

perturbation \dot{E} , and to identify the constrained gradient of the functional. To this end, we first compute the free gradient and then we discuss how to deal with the projection onto the admissible set. Then, in [Subsection 5.2](#) we will discuss the free gradient transition phase that characterizes the outer iteration level for (5.1).

5.2. The free gradient. We compute here the free gradient of F with respect to E , given a fixed ε . In order to proceed, we need a few preliminary results.

The following is a standard perturbation result for eigenvalues; see e.g. [23], where we denote by $\langle X, Y \rangle = \sum_{i,j} x_{ij} y_{ij} = \text{Tr}(X^\top Y)$ the inner product in $\mathbb{R}^{n \times n}$ that induces the Frobenius norm $\|X\| = \langle X, X \rangle^{1/2}$.

Theorem 5.1 (Derivative of simple eigenvalues). *Consider a continuously differentiable path of square symmetric matrices $A(t)$ for t in an open interval \mathcal{I} . Let $\lambda(t)$, $t \in \mathcal{I}$, be a continuous path of simple eigenvalues of $A(t)$. Let $\mathbf{x}(t)$ be the eigenvector associated to the eigenvalue $\lambda(t)$ and assume $\|\mathbf{x}(t)\| = 1$ for all t . Then λ is continuously differentiable on \mathcal{I} with the derivative (denoted by a dot)*

$$(5.3) \quad \dot{\lambda} = \mathbf{x}^\top \dot{A} \mathbf{x} = \langle \mathbf{x} \mathbf{x}^\top, \dot{A} \rangle.$$

Moreover, “continuously differentiable” can be replaced with “analytic” in the assumption and the conclusion.

Let us denote the perturbed weight matrix by $\widetilde{W}_1(t) = W_1 + \varepsilon E(t)$, and the corresponding $\widetilde{W}_0(t) = W_0(\widetilde{W}_1(t))$ and $\widetilde{W}_2(t) = W_2(\widetilde{W}_1(t))$, defined accordingly as discussed in [Section 3](#); we omit the time dependence for the perturbed matrices to simplify the notation. Since \widetilde{W}_0 , \widetilde{W}_1 and \widetilde{W}_2 are necessarily diagonal, by the chain rule we have $\dot{\widetilde{W}}_i(t) = \varepsilon \text{diag}(J_1^i \dot{E} \mathbf{1})$, where $\mathbf{1}$ is the vector of all ones, $\text{diag}(\mathbf{v})$ is the diagonal matrix with diagonal entries the vector \mathbf{v} , and J_1^i is the Jacobian matrix of the i -th weight matrix with respect to \widetilde{W}_1 , which for any $u_1 \in \mathcal{V}_1$ and $u_2 \in \mathcal{V}_i$, has entries

$$[J_1^i]_{u_1, u_2} = \frac{\partial}{\partial \widetilde{w}_1(u_1)} \widetilde{w}_i(u_2).$$

Next, in the following two lemmas, we express the time derivative of the Laplacian \overline{L}_0 and \overline{L}_1^{up} as functions of $E(t)$. The proofs of these results are straightforward and omitted for brevity. In what follows, $\text{Sym}[A]$ denotes the symmetric part of the matrix A , namely $\text{Sym}[A] = (A + A^\top)/2$.

Lemma 5.2 (Derivative of \overline{L}_0). *For the simplicial complex \mathcal{K} with the initial edges’ weight matrix W_1 and fixed perturbation norm ε , let $E(t)$ be a smooth path and $\widetilde{W}_0, \widetilde{W}_1, \widetilde{W}_2$ be corresponding perturbed weight matrices. Then,*

$$(5.4) \quad \frac{1}{2\varepsilon} \frac{d}{dt} \overline{L}_0(t) = \widetilde{W}_0^{-1} B_1 \widetilde{W}_1 \dot{E} B_1^\top \widetilde{W}_0^{-1} - \text{Sym} \left[\widetilde{W}_0^{-1} \text{diag} \left(J_1^0 \dot{E} \mathbf{1} \right) \widetilde{L}_0 \right].$$

Lemma 5.3 (Derivative of \bar{L}_1^{up}). *For the simplicial complex \mathcal{K} with the initial edges' weight matrix W_1 and fixed perturbation norm ε , let $E(t)$ be a smooth path and $\widetilde{W}_0, \widetilde{W}_1, \widetilde{W}_2$ be corresponding perturbed weight matrices. Then,*

$$(5.5) \quad \frac{1}{2\varepsilon} \frac{d}{dt} \bar{L}_1^{up}(t) = -\text{Sym} \left[\widetilde{W}_1^{-1} B_2 \widetilde{W}_2^2 B_2^\top \widetilde{W}_1^{-1} \dot{E} \widetilde{W}_1^{-1} \right] +$$

$$(5.6) \quad + \widetilde{W}_1^{-1} B_2 \widetilde{W}_2 \text{diag} \left(J_1^0 \dot{E} \mathbf{1} \right) B_2^\top \widetilde{W}_1^{-1}$$

Combining [Theorem 5.1](#) with [Lemma 5.2](#) and [Lemma 5.3](#) we obtain the following expression for the gradient of the functional.

Theorem 5.4 (The free gradient of $F(\varepsilon, E)$). *Assume the initial weight matrices W_0, W_1 and W_2 , as well as the parameters $\varepsilon > 0, \alpha > 0$ and $\mu > 0$, are given. Additionally assume that $E(t)$ is a differentiable matrix-valued function such that the first non-zero eigenvalue $\lambda_+(\varepsilon, E)$ of $\bar{L}_1^{up}(\varepsilon, E)$ and the second smallest eigenvalue $\mu_2(\varepsilon, E)$ of $\bar{L}_0(\varepsilon, E)$ are simple. Let $\widetilde{W}_0, \widetilde{W}_1, \widetilde{W}_2$ be corresponding perturbed weight matrices; then:*

$$\begin{aligned} \frac{1}{\varepsilon} \nabla_E F(\varepsilon, E)(t) = & \lambda_+(\varepsilon, E) \left[\text{Sym} \left[-\widetilde{W}_1^{-1} B_2 \widetilde{W}_2^2 B_2^\top \widetilde{W}_1^{-1} \mathbf{x}_+ \mathbf{x}_+^\top \widetilde{W}_1^{-1} \right] \right. \\ & + \text{diag} \left(J_1^2{}^\top \text{diagvec} \left(B_2^\top \widetilde{W}_1^{-1} \mathbf{x}_+ \mathbf{x}_+^\top \widetilde{W}_1^{-1} B_2 \widetilde{W}_2 \right) \right) \Big] - \\ & - \frac{\alpha}{\mu} \max \left\{ 0, 1 - \frac{\mu_2(\varepsilon, E)}{\mu} \right\} \left[B_1^\top \widetilde{W}_0^{-1} \mathbf{y}_2 \mathbf{y}_2^\top \widetilde{W}_0^{-1} B_1 \widetilde{W}_1 - \right. \\ & \left. - \text{diag} \left(J_1^0{}^\top \text{diagvec} \left(\text{Sym}[\widetilde{W}_0^{-1} \mathbf{y}_2 \mathbf{y}_2^\top \bar{L}_0] \right) \right) \right] \end{aligned}$$

where \mathbf{x}_+ is a unit eigenvector of \bar{L}_1^{up} corresponding to λ_+ , \mathbf{y}_2 is a unit eigenvector of \bar{L}_0 corresponding to μ_2 , and the operator $\text{diagvec}(X)$ returns the main diagonal of X as a vector.

Proof. To derive the expression for the gradient $\nabla_E F$, we exploit the chain rule for the time derivative: $\dot{\lambda} = \langle \frac{d}{dt} A(E(t)), \mathbf{x} \mathbf{x}^\top \rangle = \langle \nabla_E \lambda, \dot{E} \rangle$. Then it is sufficient to apply the cyclic perturbation for the scalar products of [Lemma 5.2](#) and [Lemma 5.3](#) with $\mathbf{x}_+ \mathbf{x}_+^\top$ and $\mathbf{y}_2 \mathbf{y}_2^\top$ respectively. The final transition requires the formula:

$$\langle A, \text{diag}(BE\mathbf{1}) \rangle = \left\langle \text{diag} \left(B^\top (\text{diagvec } A) \right), E \right\rangle \quad \blacksquare$$

Remark 5.5. The derivation above assumes the simplicity of both $\mu_2(\varepsilon, E)$ and $\lambda_+(\varepsilon, E)$. This assumption is not too restrictive as simplicity for these extremal eigenvalues is a generic property. We observe simplicity in all our numerical tests.

5.3. The constrained gradient system and its stationary points. In this section we are deriving from the free gradient determined in [Theorem 5.4](#) the constrained gradient of the considered functional, that is the projected gradient (with respect to the Frobenius inner product) onto the manifold $\Omega \cap \Pi_\varepsilon$, composed of perturbations E which preserve the structure of W and the unit norm constraint of E .

In order to obtain the constrained gradient system, we need to project the unconstrained gradient given by [Theorem 5.4](#) onto the feasible set and also to normalize E to preserve its unit norm. On a time interval where the set of 0-weight edges remains unchanged, the norm-unconstrained gradient is given by (a formal derivation can be established through the KKT conditions):

$$(5.7) \quad \mathbb{P}_+ G(\varepsilon, E)$$

where \mathbb{P}_+ is the non-negativity projection such that

$$[\mathbb{P}_+ X]_{ij} = \begin{cases} X_{ij}, & [W_1 + \varepsilon E]_{ij} > 0 \\ 0, & \text{otherwise} \end{cases}.$$

Further, in order to comply with the constraint $\|E(t)\|^2 = 1$, we must have

$$(5.8) \quad 0 = \frac{1}{2} \frac{d}{dt} \|E(t)\|^2 = \langle E(t), \dot{E}(t) \rangle.$$

We are thus led to the following constrained optimization problem for the admissible direction of the steepest descent.

Lemma 5.6 (Direction of steepest admissible descent). *Let $E, G \in \mathbb{R}^{n,n}$ with G given by (5.7) and $\|E\|_F = 1$. On a time interval where the set of 0-weight edges remains unchanged, the gradient system reads*

$$(5.9) \quad \dot{E}(t) = -\mathbb{P}_+ G(\varepsilon, E(t)) + \kappa \mathbb{P}_+ E(t), \quad \text{where} \quad \kappa = \frac{\langle \varepsilon, G(E(t)), \mathbb{P}_+ E(t) \rangle}{\|\mathbb{P}_+ E(t)\|^2}.$$

Proof. We need to orthogonalize $\dot{E}(t)$ with respect to $E(t)$. As usual, this can be obtained by the introduction of a linear orthogonality correction. The gradient system reads

$$(5.10) \quad \dot{E} = \mathbb{P}_+ (-G - \kappa E),$$

where κ is determined from the constraint $\langle E, \dot{E} \rangle = 0$. We then have

$$0 = \langle E, \dot{E} \rangle = \langle E, \mathbb{P}_+ (-G - \kappa E) \rangle = -\langle \mathbb{P}_+ E, G \rangle - \kappa \langle \mathbb{P}_+ E, \mathbb{P}_+ E \rangle,$$

and the result follows. ■

[Equation \(5.9\)](#) suggests that the systems goes “primarily” in the direction of the antigradient $-G(E, \varepsilon)$, thus the functional is expected to decrease along it.

Lemma 5.7 (Monotonicity). *Let $E(t)$ of unit Frobenius norm satisfy the differential equation (5.10) with G given by (5.7). Then, the functional $F_k(\varepsilon, E)(t)$ decreases monotonically with t .*

Proof. We consider first the simpler case where the non-negativity projection does not apply so that $G = G(E, \varepsilon)$ (without \mathbb{P}_+). Then

$$\begin{aligned}
 \frac{d}{dt}F(\varepsilon, E)(t) &= \left\langle \nabla_E F_k(\varepsilon, E), \dot{E} \right\rangle = \langle \varepsilon G(\varepsilon, E(t)), -G(\varepsilon, E(t)) + \kappa E(t) \rangle = \\
 &= -\varepsilon \|G(\varepsilon, E)\|^2 + \varepsilon \frac{\langle G(\varepsilon, E), E \rangle}{\langle E, E \rangle} \langle G(\varepsilon, E), E \rangle = \\
 (5.11) \quad &= \varepsilon \left(-\|G(\varepsilon, E)\|^2 + \frac{|\langle G(\varepsilon, E), E \rangle|^2}{\|E\|^2} \right) \leq 0
 \end{aligned}$$

where the final estimate is given by the Cauchy-Bunyakovsky-Schwarz inequality. The derived inequality holds on the time interval without the change in the support of \mathbb{P}_+ (so that no new edges are prohibited by the non-negativity projection). ■

As a direct consequence, we observe that the stationary points of the differential equation (5.10) are characterized as follows.

Theorem 5.8 (Stationary points). *Let E_\star be an admissible perturbation with $\|E_\star\|_F = 1$ be such that*

- (i) *The eigenvalue $\lambda_+(\varepsilon, E)$ is simple at $E = E_\star$ and depends continuously on E in a neighborhood of E_\star .*
- (ii) *Penalization is not active, i.e. $\mu_2(\varepsilon, E) > \mu$.*
- (iii) *The gradient $G(\varepsilon, E_\star)$ is nonzero.*

Let $E(t)$ be the solution of (5.10) passing through E_\star . Then the following are equivalent:

1. $\frac{d}{dt}F(\varepsilon, E(t)) = 0$.
2. $\dot{E} = 0$.
3. E_\star is a real multiple of $G(\varepsilon, E_\star)$.

Proof. It is immediate to see that 3. implies 2., which implies 1. The proof is concluded noting that (5.11) shows that 1. implies 3 by the strict form of Cauchy-Bunyakovsky-Schwarz inequality. ■

5.4. Free Gradient Transition in the Outer Level. The optimization problem in the *inner level* is non-convex due to the non-convexity of the functional $F(\varepsilon, E)$. Hence, for a given ε , the computed minimizer $E(\varepsilon)$ may depend on the initial guess $E_0 = E_0(\varepsilon)$.

The effects of the initial choice are particularly important upon the transition $\hat{\varepsilon} \rightarrow \varepsilon = \hat{\varepsilon} + \Delta\varepsilon$ between constrained inner levels: given reasonably small $\Delta\varepsilon$, one should expect relatively close optimizers $E(\hat{\varepsilon})$ and $E(\varepsilon)$, and, hence, the initial guess $E_0(\varepsilon)$ being close to and dependent on $E(\varepsilon)$.

This choice, which seems very natural, determines however a discontinuity

$$F(\hat{\varepsilon}, E(\hat{\varepsilon})) \neq F(\varepsilon, E(\hat{\varepsilon})),$$

which may prevent the expected monotonicity property with respect to ε in the (likely unusual case) where $F(\hat{\varepsilon}, E(\hat{\varepsilon})) < F(\varepsilon, E(\hat{\varepsilon}))$. This may happen in particular when $\Delta\varepsilon$ is not taken small; since the choice of $\Delta\varepsilon$ is driven by a Newton-like iteration we are interested in finding a way to prevent this situation and making the whole iterative method more robust. The goal

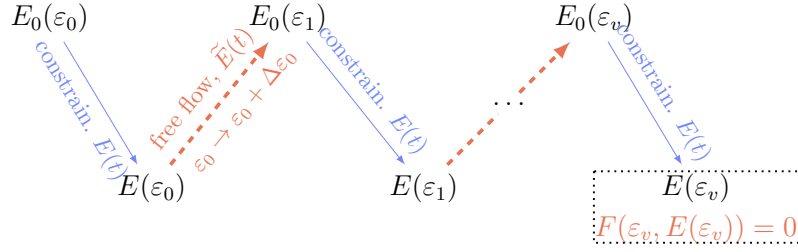


Figure 5. The scheme of alternating constrained (blue) and free gradient (red) flows. Each stage inherits the final iteration of the previous stage as initial $E_0(\varepsilon_i)$ or $\tilde{E}_0(\varepsilon_i)$ respectively. The scheme alternates until the target functional vanishes ($F(\varepsilon, E) = 0$).

is that of guaranteeing monotonicity of the functional both with respect to time and with respect to ε .

When in the outer iteration we increase ε from a previous value $\hat{\varepsilon} < \varepsilon$, we have the problem of choosing a suitable initial value for the constrained gradient system (5.9), such that at the stationary point $E(\hat{\varepsilon})$ we have $F(\hat{\varepsilon}, E(\hat{\varepsilon})) < F(\varepsilon, E(\varepsilon))$ (which we assume both positive, that is on the left of the value ε^* which identifies the closest zero of the functional).

In order to maintain monotonicity with respect to time and also with respect to ε , it is convenient to start to look at the optimization problem with value ε , with the initial datum $\delta W_1 = \hat{\varepsilon} E(\hat{\varepsilon})$ of norm $\hat{\varepsilon} < \varepsilon$.

This means we have essentially to optimize with respect to the inequality constraint $\|\delta W_1\|_F \leq \varepsilon$, or equivalently solve the problem (now with inequality constrain on $\|E\|_F$):

$$E(\varepsilon) = \arg \min_{E \in \Omega, \|E\|_F \leq 1} F(\varepsilon, E)$$

The situation changes only slightly from the one discussed above. If $\|E\|_F < 1$, every direction is admissible, and the direction of the steepest descent is given by the negative gradient. So we choose the free gradient flow

$$(5.12) \quad \dot{E} = -\mathbb{P}_+ G(\varepsilon, E(t)) \quad \text{as long as } \|E(t)\|_F < 1.$$

When $\|E(t)\|_F = 1$, then there are two possible cases. If $\langle \mathbb{P}_+ G(\varepsilon, E), E \rangle \geq 0$, then the solution of (5.12) has

$$\frac{d}{dt} \|E(t)\|_F^2 = 2 \langle \dot{E}, E \rangle = -2 \langle \mathbb{P}_+ G(\varepsilon, E(t)), E \rangle \leq 0,$$

and hence the solution of (5.12) remains of Frobenius norm at most 1.

Otherwise, if $\langle \mathbb{P}_+ G(\varepsilon, E), E \rangle < 0$, the admissible direction of steepest descent is given by the right-hand side of (5.9), i.e. $-\mathbb{P}_+ G(\varepsilon, E) + \kappa E$, $\kappa = \frac{\langle G(\varepsilon, E), \mathbb{P}_+ E \rangle}{\|\mathbb{P}_+ E\|^2}$ and so we choose that differential equation to evolve E . The situation can be summarized as taking, if $\|E(t)\|_F = 1$,

$$(5.13) \quad \dot{E} = -\mathbb{P}_+ G(\varepsilon, E) + \mu E \quad \text{with } \mu = \min(0, \kappa)$$

with $\kappa = \frac{\langle G(\varepsilon, E), \mathbb{P}_+ E \rangle}{\|\mathbb{P}_+ E\|^2}$. Along the solutions of (5.13), the functional F decays monotonically, and stationary points of (5.13) with $\mathbb{P}_+ G(\varepsilon, E(t)) \neq 0$ are characterized, by the same

Algorithm 6.1 Pseudo-code of the complete constrained- and free-gradient flow.

Require: initial edge perturbation guess E_0 ; initial $\varepsilon_0 > 0$; ε -stepsize $\Delta\varepsilon > 0$; bounds α_* , α^* for the α -phase;

- 1: $\alpha, E \leftarrow \text{AlphaPhase}(E_0, \varepsilon_0, \alpha_*, \alpha^*)$ ▷ for details see [Section 7](#)
- 2: **while** $|F(\varepsilon, E)| < 10^{-6}$ **do**
- 3: $\varepsilon \leftarrow \varepsilon + \Delta\varepsilon$
- 4: $E \leftarrow \frac{\varepsilon}{\varepsilon + \Delta\varepsilon} E$ ▷ before the free gradient $\|E\| < 1$
- 5: $E_i \leftarrow \text{FreeGradientFlow}(E, \Delta\varepsilon, \varepsilon)$ ▷ see [Subsection 5.4](#)
- 6: $E \leftarrow \text{ConstrainedGradientFlow}(E, \varepsilon)$ ▷ see [Section 6](#)
- 7: **end while**

arguments used before, as

$$(5.14) \quad E \text{ is a negative real multiple of } \mathbb{P}_+ G(\varepsilon, E(t)).$$

If it can be excluded that the gradient $\mathbb{P}_+ G(\varepsilon, E(t))$ vanishes at an optimizer, it can thus be concluded that the optimizer of the problem with inequality constraints is a stationary point of the gradient flow (5.9) for the problem with equality constraints.

Remark 5.9. As a result, $F(\varepsilon, E(t))$ monotonically decreases both with respect to time t and to the value of the norm ε , when $\varepsilon \leq \varepsilon^*$.

6. Algorithm details. In [Algorithm 6.1](#) we provide the pseudo-code of the whole bi-level procedure. The initial “ α -phase” is used to choose an appropriate value for the regularization parameter α . In order to avoid the case in which the penalizing term on the right-hand side of (4.2) dominates the loss $F(\varepsilon, E(t))$ in the early stages of the descent flow, we select α by first running such an initial phase, prior to the main alternated constrained/free gradient loop. In this phase, we fix a small $\varepsilon = \varepsilon_0$ and run the constrained gradient integration for an initial $\alpha = \alpha_*$. After the computation of a local optimum E_* , we then increase α and rerun for the same ε_0 with E_* as starting point. We iterate until no change in E_* is observed or until α reaches an upper bound α^* .

The resulting value of α and E_* are then used in the main loop where we first increase ε by the chosen step size, we rescale E_i by $0 < \varepsilon/(\varepsilon + \Delta\varepsilon) < 1$, and then we perform the free gradient integration described in [Subsection 5.4](#) until we reach a new point E_i on the unit sphere $\|E_i\| = 1$. Then, we perform the inner constrained gradient step by integrating [Equation \(5.9\)](#), iterating the following two-step norm-corrected Euler scheme:

$$(6.1) \quad \begin{cases} E_{i+1/2} = E_i - h_i (\mathbb{P}_+ G(E_i, \varepsilon) - \kappa_i \mathbb{P}_+ E_i) . \\ E_{i+1} = \mathbb{P}_{\Pi_\varepsilon} E_{i+1/2} / \|\mathbb{P}_{\Pi_\varepsilon} E_{i+1/2}\| \end{cases}$$

where the second step is necessary to numerically guarantee the Euler integration remains in the set of admissible flows since the discretization does not conserve the norm and larger steps h_i may violate the non-negativity of the weights.

In both the free and constrained integration phases, since we aim to obtain the solution at $t \rightarrow \infty$ instead of the exact trajectory, we favor larger steps h_i given that the established

monotonicity is conserved. Specifically, if $F(\varepsilon, E_{i+1}) < F(\varepsilon, E_i)$, then the step is *accepted* and we set $h_{i+1} = \beta h_i$ with $\beta > 1$; otherwise, the step is *rejected* and repeated with a smaller step $h_i \leftarrow h_i/\beta$.

Remark 6.1. The step acceleration strategy described above, where βh_i is immediately increased after one accepted step, may lead to “oscillations” between accepted and rejected steps in the event the method would prefer to maintain the current step size h_i . To avoid this potential issue, in our experiments we actually increase the step length after two consecutive accepted steps. Alternative step-length selection strategies are also possible, for example, based on Armijo’s rule or non-monotone stabilization techniques [20].

Remark 6.2. When the weight of an edge e is moved to zero, we are formally reducing the initial complex \mathcal{K} to a smaller $\tilde{\mathcal{K}}$ with $\mathcal{V}_1(\tilde{\mathcal{K}}) = \tilde{\mathcal{V}}_1 = \mathcal{V}_1 \setminus \{e\}$. While the Hodge Laplacian of the new $\tilde{\mathcal{K}}$ should have a smaller dimension than the initial one, in our perturbative approach, we want to maintain the dimension of \bar{L}_1 unchanged so as to be able to explore the set of possible perturbations $\Omega(\varepsilon) \cap \Pi(W_1)$ in a continuous way. While this may create a complication in the general unweighted setting, as it might give rise to an almost-zero row in B_1 and thus a degenerate almost-zero entry in $\sigma(L_1^{up})$ which does not correspond to a different homology, we emphasize that in our weighted set-up, this sort of faux edges are automatically ignored. In fact, in our model, the weights of the 2-simplicies W_2 evolve as a function of the edge weights W_1 as in (3.1). Thus, when an entry of W_1 approaches zero, the corresponding entries of W_2 approach 0 with the same order, and the weight normalization in the definition of \bar{B}_1 prevents the formation of zero rows.

6.1. Computational costs. Each step of either the free or the constrained flows requires one step of explicit Euler integration along the anti-gradient $-\nabla_E F(\varepsilon, E(t))$. As discussed in Section 5, the construction of such a gradient requires several sparse and diagonal matrix-vector multiplications as well as the computation of the smallest nonzero eigenvalue of both $\bar{L}_1^{up}(\varepsilon, E)$ and $\bar{L}_0(\varepsilon, E)$. The latter two represent the major computational requirements of the numerical procedure. Fortunately, as both matrices are of the form $A^\top A$, with A being either of the two boundary or co-boundary operators \bar{B}_2 and \bar{B}_1^\top , we have that both the two eigenvalue problems boil down to a problem of the form

$$\min_{\mathbf{x} \perp \ker A} \frac{\|A\mathbf{x}\|}{\|\mathbf{x}\|}$$

i.e., the computation of the smallest singular value of the sparse matrix A . This problem can be approached by a sparse singular value solver based on a Krylov subspace scheme for the pseudo inverse of $A^\top A$. In practice, we implement the pseudo inversion by solving the corresponding least squares problems

$$\min_{\mathbf{x}} \|\bar{L}_1^{up}(\varepsilon, E)\mathbf{x} - \mathbf{b}\|, \quad \min_{\mathbf{x}} \|\bar{L}_0(\varepsilon, E)\mathbf{x} - \mathbf{b}\|,$$

which, in our experiments, we solved using the least square minimal-residual method (LSMR) from [15]. This approach allows us to use a preconditioner for the normal equation corresponding to the least square problem. For simplicity, in our tests we used a constant preconditioner computed by means of an incomplete Cholesky factorization of the initial unperturbed \bar{L}_1^{up} , or

\bar{L}_0 . Possibly, much better performance can be achieved with a tailored preconditioner that is efficiently updated throughout the matrix flow. We also note that the eigenvalue problem for the graph Laplacian $\bar{L}_0(\varepsilon, E)$ may be alternatively approached by a combinatorial multigrid strategy [30]. However, designing a suitable preconditioning strategy goes beyond the scope of this work and will be the subject of future investigations.

7. Numerical experiments. In this section, we provide several synthetic and real-world example applications of the proposed stability algorithms. The code for all the examples is available at <https://github.com/COMPiLELab/HOLaGraF>. All experiments are run until the global stopping criterion $|F(\varepsilon, E(t))| < 10^{-6}$ is met and the parameters μ and α are chosen as follows. Concerning μ , since the effect of weight perturbations on $\mu_2(\varepsilon, E)$ diminishes with the growth of the network, $F(\varepsilon, E)$ becomes less sensitive to it. Thus, in the computations we set $\mu = 0.75\mu_2$, where μ_2 is the smallest nonzero eigenvalue of the initial Laplacian \bar{L}_0 . As for α , we run the α -phase described in Section 6 with parameters $\varepsilon_0 = 10^{-3}$, $\alpha_* = 1$ and $\alpha^* = 100$.

7.1. Illustrative Example. We consider here a small example of a simplicial complex \mathcal{K} of order 2 consisting of eight 0-simplicies (vertices), twelve 1-simplicies (edges), four 2-simplicies $\mathcal{V}_2 = \{[1, 2, 3], [1, 2, 8], [4, 5, 6], [5, 6, 7]\}$ and one corresponding hole $[2, 3, 4, 5]$, hence, $\beta_1 = 1$. By design, the dimensionality of the homology group $\bar{\mathcal{H}}_1$ can be increased only by eliminating edges $[1, 2]$ or $[5, 6]$; for the chosen weight profile $w_1([1, 2]) > w_1([5, 6])$, hence, the method should converge to the minimal perturbation norm $\varepsilon = w_1([5, 6])$ by eliminating the edge $[5, 6]$.

The exemplary run of the optimization framework in time is shown on Figure 6. The top panel of Figure 6 provides the continued flow of the target functional $F(\varepsilon, E(t))$ consisting of the initial α -phase (in green) and alternated constrained (in blue) and free gradient (in orange) stages. As stated above, $F(\varepsilon, E(t))$ is strictly monotonic along the flow since the support of \mathbb{P}_+ does not change. Since the initial setup is not pathological with respect to the connectivity, the initial α -phase essentially reduces to a single constrained gradient flow and terminates after one run with $\alpha = \alpha_*$. The constrained gradient stages are characterized by a slow changing $E(t)$, which is essentially due to the flow performing small adjustments to find the correct rotation on the unit sphere, whereas the free gradient stage quickly decreases the target functional.

The second panel shows the behaviour of first non-zero eigenvalue $\lambda_+(\varepsilon, E(t))$ (solid line) of $\bar{L}_1^{up}(\varepsilon, E(t))$ dropping through the ranks of $\sigma(\bar{L}_1(\varepsilon, E(t)))$ (semi-transparent); similar to the case of the target functional $F(\varepsilon, E(t))$, $\lambda_+(\varepsilon, E(t))$ monotonically decreases. The rest of the eigenvalues exhibit only minor changes, and the rapidly changing λ_+ successfully passes through the connectivity threshold μ (dotted line).

The third and the fourth panels show the evolution of the norm of the perturbation $\|E(t)\|$ and the perturbation $E(t)$ itself, respectively. The norm $\|E(t)\|$ is conserved during the constrained-gradient and the α - stages; these stages correspond to the optimization of the perturbation shape, as shown by the small positive values at the beginning of the bottom panel which eventually vanish. During the free gradient integration the norm $\|E(t)\|$ increases, but the relative change of the norm declines with the growth of ε_i to avoid jumping over the smallest possible ε . Finally, due to the simplicity of the complex, the edge we want to eliminate, 56, dominates the flow from the very beginning (see bottom panel); such a clear

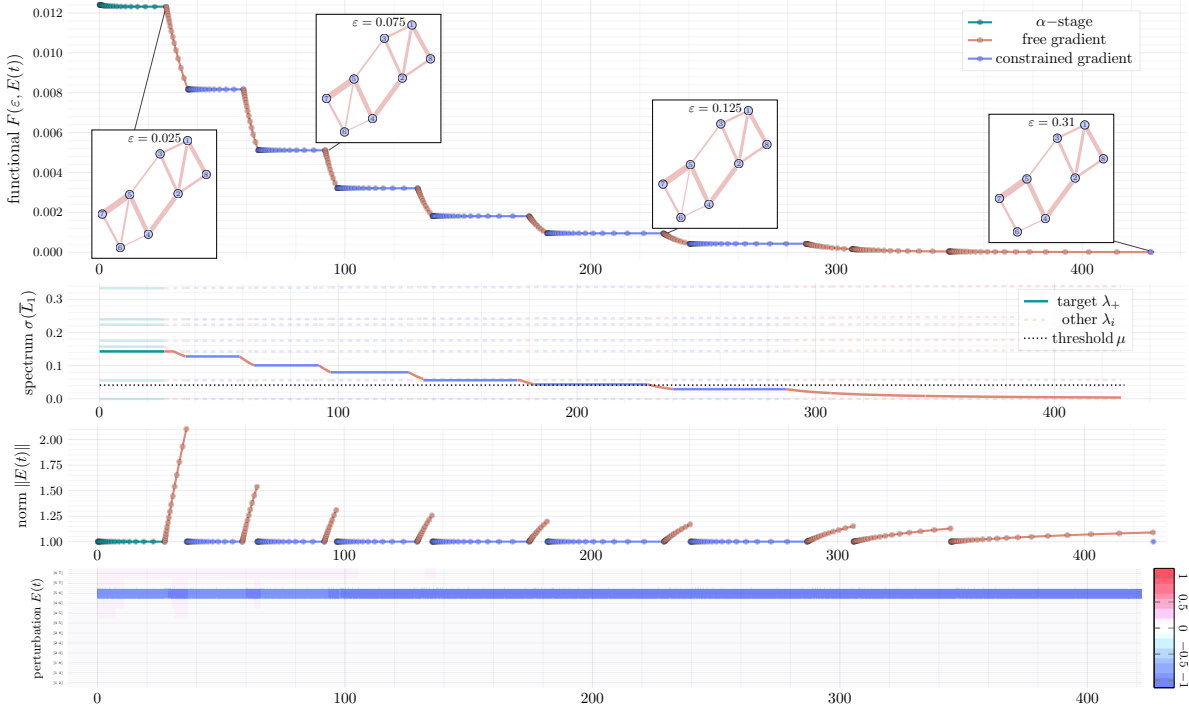


Figure 6. Illustrative run of the framework determining the topological stability: the top pane — the flow of the functional $F(\varepsilon, E(t))$; the second pane — the flow of $\sigma(L_1)$, λ_+ is highlighted; third pane — the change of the perturbation norm $\|E(t)\|$; the bottom pane — the heatmap of the perturbation profile $E(t)$.

pattern persists only in small examples, whereas for large networks the perturbation profile is initially spread out among all the edges.

7.2. Triangulation Benchmark. To provide more insight into the computational behavior of the method, we synthesize here an almost planar graph dataset. Namely, we assume N uniformly sampled vertices on the unit square with a network built by the Delaunay triangulation; then, edges are randomly added or erased to obtain the sparsity ν (so that the graph has $\frac{1}{2}\nu N(N-1)$ edges overall). An order-2 simplicial complex $\mathcal{K} = (\mathcal{V}_0, \mathcal{V}_1, \mathcal{V}_2)$ is then formed by letting \mathcal{V}_0 be the generated vertices, \mathcal{V}_1 the edges, and \mathcal{V}_2 every 3-clique of the graph; edges' weights are sampled uniformly between $1/4$ and $3/4$, namely $w_1(e_i) \sim U[\frac{1}{4}, \frac{3}{4}]$.

An example of such triangulation is shown in Figure 7a; here $N = 8$ and edges $[6, 8]$ and $[2, 7]$ were eliminated to achieve the desired sparsity.

We sample networks with a varying number of vertices $N = 10, 16, 22, 28$ and varying sparsity pattern $\nu = 0.35, 0.5$ which determine the number of edges in the output as $m = \nu \frac{N(N-1)}{2}$. Due to the highly randomized procedure, topological structures of a sampled graph with a fixed pair of parameters may differ substantially, so 10 networks with the same (N, ν) pair are generated. For each network, the working time (without considering the sampling itself) and the resulted perturbation norm ε , and are reported in Figure 7b and Figure 7c, respectively. As anticipated in Subsection 6.1, we show the performance of two implementations of the method, one based on LSMR and one based on LSMR preconditioned

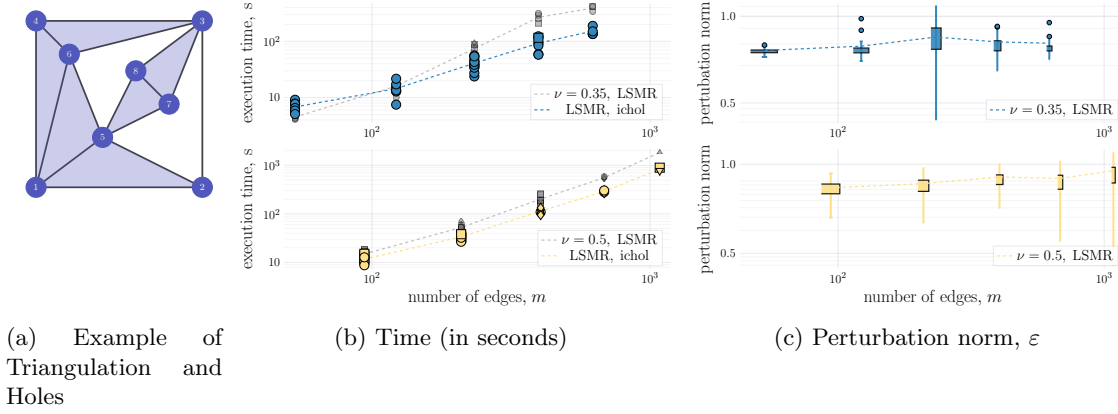


Figure 7. Benchmarking Results on the Synthetic Triangulation Dataset: varying sparsities $\nu = 0.35, 0.5$ and $N = 16, 22, 28, 34, 40$; each network is sampled 10 times. Shapes correspond to the number of eliminated edges in the final perturbation: 1 : \circ , 2 : \square , 3 : \diamond , 4 : \triangle . For each pair (ν, N) , the un-preconditioned and Cholesky-preconditioned execution times are shown.

by using the incomplete Cholesky factorization of the initial matrices. We observe that,

- the computational cost of the whole procedure lies between $\mathcal{O}(m^2)$ and $\mathcal{O}(m^3)$
- denser structures, with a higher number of vertices, result in the higher number of edges being eliminated; at the same time, even most dense cases still can exhibit structures requiring the elimination of a single edge, showing that the flow does not necessarily favor multi-edge optima;
- the required perturbation norm ε is growing with the size of the graph, Figure 7c, but not too fast: it is expected that denser networks would require larger ε to create a new hole; at the same time if the perturbation were to grow drastically with the sparsity ν , it would imply that the method tries to eliminate sufficiently more edges, a behavior that resembles convergence to a sub-optimal perturbation;
- preconditioning with a constant incomplete Cholesky multiplier, computed for the initial Laplacians, provides a visible execution time gain for medium and large networks. Since the quality of the preconditioning deteriorates as the flow approaches the minimizer (as a non-zero eigenvalue becomes 0), it is worth investigating the design of a preconditioner for the up-Laplacian that can be efficiently updated.

7.3. Transportation Networks. Finally, we provide an application to real-world examples based on city transportation networks. We consider networks for Bologna, Anaheim, Berlin Mitte, and Berlin Tiergarten; each network consists of nodes — intersections/public transport stops — connected by edges (roads) and subdivided into zones; for each road the free flow time, length, speed limit are known; moreover, the travel demand for each pair of nodes is provided through the dataset of recorded trips. All the datasets used here are publicly available at <https://github.com/bstabler/TransportationNetworks>; Bologna network is provided by the Physic Department of the University of Bologna (enriched through the Google Maps API <https://developers.google.com/maps>).

The regularity of city maps naturally lacks 3-cliques, hence forming the simplicial complex

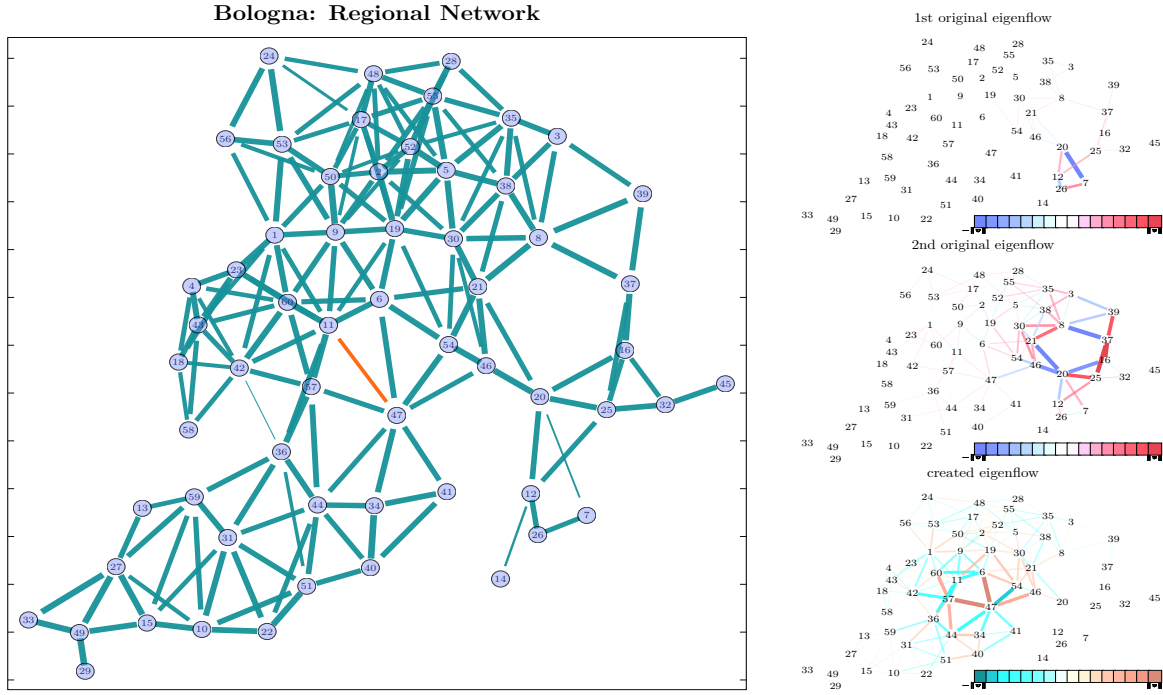


Figure 8. Example of the Transportation Network for Bologna. Left pane: original zone graph where the width of edges corresponds to the weight, to-be-eliminated edge is colored in red. Right pane: eigenflows, original and created; color and width correspond to the magnitude of entries.

based on triangulations as done before frequently leads to trivial outcomes. Instead, here we “lift” the network to city zones, thus more effectively grouping the nodes in the graph. Specifically:

1. we consider the completely connected graph where the nodes are zones in the city/region;
2. the free flow time between two zones is temporarily assigned as a weight of each edge: the time is as the shortest path between the zones (by the classic Dijkstra algorithm) on the initial graph;
3. similarly to what is done in the filtration used for persistent homology, we filter out excessively distant nodes; additionally, we exclude the longest edges in each triangle in case it is equal to the sum of two other edges (so the triangle is degenerate and the trip by the longest edge is always performed through to others);
4. finally, we use the travel demand as an actual weight of the edges in the final network; travel demands are scaled *logarithmically* via the transformation $w_i \mapsto \log_{10} \left(\frac{w_i}{0.95 \min w_i} \right)$; see the example on the left panel of [Figure 8](#).

Given the definition of weights in the network, high instability (corresponding to small perturbation norm ε) implies structural phenomena around the “almost-hole”, where the faster and shorter route is sufficiently less demanded.

In the case of Bologna, [Figure 8](#), the algorithm eliminates the edge [11, 47] (Casalecchio

Table 1

Topological instability of the transportation networks: filtered zone networks with the corresponding perturbation norm ε and its percentile among $w_1(\cdot)$ profile. For each simplicial complex the number of nodes, edges and triangles in $\mathcal{V}_2(\mathcal{K})$ are provided alongside the initial number of holes β_1 . The results of the algorithm consist of the perturbation norm, ε , computation time, and approximate percentile p .

	network			β_1	logarithmic weights		
	n	m	Δ		time	ε	p
Bologna	60	175	171	2	2.43s	0.65	0.003
					[11, 47] (4^{th} smallest)		
Anaheim	38	159	221	1	5.39s	0.57	0.003
					[10, 29] (11^{th} smallest)		
Berlin-Tiergarten	26	63	55	0	2.46s	1.18	0.015
					[6, 16] (20^{th} smallest)		
Berlin-Mitte	98	456	900	1	127s	0.887	0.0016
					[57, 87] (6^{th}), [58, 87], (17^{th})		

di Reno – Pianoro) creating a new hole $6 - 11 - 57 - 47$. We also provide examples of the eigenflows in the kernel of the Hodge Laplacian (original and additional perturbed): original eigenvectors correspond to the circulations around holes $7 - 26 - 12 - 20$ and $8 - 21 - 20 - 16 - 37$ non-locally spread in the neighborhood [29].

The results for four different networks are summarized in the Table 1; p mimics the percentile, $\varepsilon / \sum_{e \in \mathcal{V}_1} w_i(e)$, showing the overall small perturbation norm contextually. At the same time, we emphasize that except Bologna (which is influenced by the geographical topology of the land), the algorithm does not choose the smallest weight possible; indeed, given our interpretation of the topological instability, the complex for Berlin-Tiergarten is stable and the transportation network is effectively constructed.

8. Discussion. In the current work, we formulate the notion of k -th order topological stability of a simplicial complex \mathcal{K} as the smallest data perturbation required to create one additional k -th order hole in \mathcal{K} . By introducing an appropriate weighting and normalization, the stability is reduced to a matrix nearness problem solved by a bi-level optimization procedure. Despite the highly nonconvex landscape, our proposed procedure alternating constrained and free gradient steps yields a monotonic descending scheme. Our experiments show that this approach is generally successful in computing the minimal perturbation increasing $\beta_1(\varepsilon, E)$, even for potentially difficult cases, as the one proposed in Subsection 7.1.

For simplicity, here we limit our attention to the smallest perturbation that introduces only one new hole. However, a simple modification may be employed to address the case of the introduction of m new holes: include the sum of m nonzero eigenvalues of $L_1^{up}(\varepsilon, E)$ rather than just the first one in the spectral functional (4.2). We also remark that, due to the spectral inheritance principle Theorem 2.7, the proposed framework for $\overline{\mathcal{H}}_1$ can be in principle extended to a general $\overline{\mathcal{H}}_k$; however, this extension requires nontrivial considerations on the data modification procedure and on the numerical linear algebra tools, as a nontrivial topology of higher-order requires a much denser network.

Different improvements are possible in terms of numerical implementation, including investigating the use of more sophisticated (e.g. implicit) integrators for the gradient flow system (Equation (5.9)), which would additionally require the use of higher-order derivatives

of $\lambda_+(\varepsilon, E)$. Moreover, as already mentioned in Subsection 6.1, the numerical method for the computation of the small singular values would benefit from the use of an efficient preconditioner that can be effectively updated throughout the flow. Investigations in this direction are in progress and will be the subject of future work.

REFERENCES

- [1] K. M. ALTENBURGER AND J. UGANDER, *Monophily in social networks introduces similarity among friends-of-friends*, Nature human behaviour, 2 (2018), pp. 284–290.
- [2] E. ANDREOTTI, D. EDELMANN, N. GUGLIELMI, AND C. LUBICH, *Graph partitioning using matrix differential equations*, 2017, <https://doi.org/10.48550/ARXIV.1712.05993>.
- [3] F. ARRIGO, D. J. HIGHAM, AND F. TUDISCO, *A framework for second-order eigenvector centralities and clustering coefficients*, Proceedings of the Royal Society A, 476 (2020), p. 20190724.
- [4] F. BATTISTON, G. CENCETTI, I. IACOPINI, V. LATORA, M. LUCAS, A. PATANIA, J.-G. YOUNG, AND G. PETRI, *Networks beyond pairwise interactions: Structure and dynamics*, Physics Reports, 874 (2020), pp. 1–92, <https://doi.org/10.1016/j.physrep.2020.05.004>.
- [5] A. R. BENSON, *Three hypergraph eigenvector centralities*, SIAM Journal on Mathematics of Data Science, 1 (2019), pp. 293–312.
- [6] A. R. BENSON, R. ABEBE, M. T. SCHAUB, A. JADBABAIE, AND J. KLEINBERG, *Simplicial closure and higher-order link prediction*, Proceedings of the National Academy of Sciences, 115 (2018), pp. E11221–E11230.
- [7] A. R. BENSON, D. F. GLEICH, AND J. LESKOVEC, *Higher-order organization of complex networks*, Science, 353 (2016), pp. 163–166, <https://doi.org/10.1126/science.aad9029>.
- [8] A. R. BENSON, D. F. GLEICH, AND J. LESKOVEC, *Higher-order organization of complex networks*, Science, 353 (2016), pp. 163–166.
- [9] C. BICK, E. GROSS, H. A. HARRINGTON, AND M. T. SCHAUB, *What are higher-order networks?*, CoRR, abs/2104.11329 (2021), <https://arxiv.org/abs/2104.11329>.
- [10] Y.-C. CHEN AND M. MEILA, *The decomposition of the higher-order homology embedding constructed from the k -Laplacian*, Advances in Neural Information Processing Systems, 34 (2021), pp. 15695–15709.
- [11] Y.-C. CHEN, M. MEILÄ, AND I. G. KEVREKIDIS, *Helmholtzian eigenmap: Topological feature discovery and edge flow learning from point cloud data*, rXiv:2103.07626, (2021), <https://doi.org/10.48550/ARXIV.2103.07626>.
- [12] S. EBELI AND G. SPREEMANN, *A notion of harmonic clustering in simplicial complexes*, in 2019 18th IEEE International Conference On Machine Learning And Applications (ICMLA), IEEE, 2019, pp. 1083–1090.
- [13] E. ESTRADA AND D. J. HIGHAM, *Network properties revealed through matrix functions*, SIAM review, 52 (2010), pp. 696–714.
- [14] M. FIEDLER, *Laplacian of graphs and algebraic connectivity*, Banach Center Publications, 25 (1989), pp. 57–70.
- [15] D. C.-L. FONG AND M. SAUNDERS, *Lsmr: An iterative algorithm for sparse least-squares problems*, SIAM Journal on Scientific Computing, 33 (2011), pp. 2950–2971.
- [16] S. FORTUNATO AND D. HRIC, *Community detection in networks: A user guide*, Physics reports, 659 (2016), pp. 1–44.
- [17] K. FOUNTOLAKIS, P. LI, AND S. YANG, *Local hyper-flow diffusion*, Advances in Neural Information Processing Systems, 34 (2021), pp. 27683–27694.
- [18] N. E. FRIEDKIN, *Theoretical foundations for centrality measures*, American journal of Sociology, 96 (1991), pp. 1478–1504.
- [19] J. GHADERI AND R. SRIKANT, *Opinion dynamics in social networks with stubborn agents: Equilibrium and convergence rate*, Automatica, 50 (2014), pp. 3209–3215.
- [20] L. GRIPPO, F. LAMPARIELLO, AND S. LUCIDI, *A class of nonmonotone stabilization methods in unconstrained optimization*, Numerische Mathematik, 59 (1991), pp. 779–805.
- [21] N. GUGLIELMI AND C. LUBICH, *Matrix nearness problems and eigenvalue optimization*, in preparation,

- 2022.
- [22] D. HORAK AND J. JOST, *Spectra of combinatorial Laplace operators on simplicial complexes*, Advances in Mathematics, 244 (2013), pp. 303–336.
 - [23] R. A. HORN AND C. R. JOHNSON, *Matrix Analysis*, Cambridge University Press, 1990.
 - [24] L.-H. LIM, *Hodge Laplacians on graphs*, SIAM Review, (2015), pp. 685–715.
 - [25] A. MUHAMMAD AND M. EGERSTEDT, *Control using higher order laplacians in network topologies*, in Proc. of 17th International Symposium on Mathematical Theory of Networks and Systems, Citeseer, 2006, pp. 1024–1038.
 - [26] B. NETTASINGHE, V. KRISHNAMURTHY, AND K. LERMAN, *Diffusion in social networks: Effects of monophilic contagion, friendship paradox and reactive networks*, IEEE Transactions on Network Science and Engineering, (2019).
 - [27] M. E. NEWMAN, *Finding community structure in networks using the eigenvectors of matrices*, Physical review E, 74 (2006), p. 036104.
 - [28] N. OTTER, M. A. PORTER, U. TILLMANN, P. GRINDROD, AND H. A. HARRINGTON, *A roadmap for the computation of persistent homology*, EPJ Data Science, 6 (2017), pp. 1–38.
 - [29] M. T. SCHAUB, A. R. BENSON, P. HORN, G. LIPPNER, AND A. JADBABAIE, *Random walks on simplicial complexes and the normalized Hodge 1-Laplacian*, SIAM Review, 62 (2020), pp. 353–391.
 - [30] D. A. SPIELMAN AND S.-H. TENG, *Nearly linear time algorithms for preconditioning and solving symmetric, diagonally dominant linear systems*, SIAM Journal on Matrix Analysis and Applications, 35 (2014), pp. 835–885.
 - [31] S. H. STROGATZ, *From kuramoto to crawford: exploring the onset of synchronization in populations of coupled oscillators*, Physica D: Nonlinear Phenomena, 143 (2000), pp. 1–20.
 - [32] F. TUDISCO, F. ARRIGO, AND A. GAUTIER, *Node and layer eigenvector centralities for multiplex networks*, SIAM Journal on Applied Mathematics, 78 (2018), pp. 853–876.
 - [33] F. TUDISCO, A. R. BENSON, AND K. PROKOPCHIK, *Nonlinear higher-order label spreading*, in Proceedings of the Web Conference 2021, 2021, pp. 2402–2413.
 - [34] F. TUDISCO AND M. HEIN, *A nodal domain theorem and a higher-order cheeger inequality for the graph p -laplacian*, (2016), <https://arxiv.org/abs/1602.05567>.
 - [35] F. TUDISCO AND D. J. HIGHAM, *Core-periphery detection in hypergraphs*, SIAM Journal on Mathematics of Data Science, (to appear).
 - [36] F. TUDISCO, P. MERCADO, AND M. HEIN, *Community detection in networks via nonlinear modularity eigenvectors*, SIAM Journal on Applied Mathematics, 78 (2018), pp. 2393–2419.
 - [37] S. VIGNA, *Spectral ranking*, Network Science, 4 (2016), pp. 433–445.